



저작자표시-비영리-변경금지 2.0 대한민국

이용자는 아래의 조건을 따르는 경우에 한하여 자유롭게

- 이 저작물을 복제, 배포, 전송, 전시, 공연 및 방송할 수 있습니다.

다음과 같은 조건을 따라야 합니다:



저작자표시. 귀하는 원저작자를 표시하여야 합니다.



비영리. 귀하는 이 저작물을 영리 목적으로 이용할 수 없습니다.



변경금지. 귀하는 이 저작물을 개작, 변형 또는 가공할 수 없습니다.

- 귀하는, 이 저작물의 재이용이나 배포의 경우, 이 저작물에 적용된 이용허락조건을 명확하게 나타내어야 합니다.
- 저작권자로부터 별도의 허가를 받으면 이러한 조건들은 적용되지 않습니다.

저작권법에 따른 이용자의 권리는 위의 내용에 의하여 영향을 받지 않습니다.

이것은 [이용허락규약\(Legal Code\)](#)을 이해하기 쉽게 요약한 것입니다.

[Disclaimer](#)

Master's Thesis

**A POROUS MEMBRANE-INTEGRATED PMMA
MICROFLUIDIC DEVICE FOR RELIABLE
CYTOTOXICITY TESTS.**

Nguyen Thi Phuong Thao

Department of Biomedical Engineering
(Biomedical Engineering)

Ulsan National Institute of Science and Technology

2021

A POROUS MEMBRANE-INTEGRATED PMMA MICROFLUIDIC DEVICE FOR RELIABLE CYTOTOXICITY TESTS

Nguyen Thi Phuong Thao

Department of Biomedical Engineering
(Biomedical Engineering)

Ulsan National Institute of Science and Technology

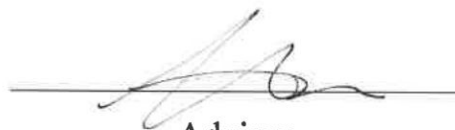
**A porous membrane-integrated PMMA microfluidic
device for reliable cytotoxicity tests.**

A thesis/dissertation submitted to UNIST
in partial fulfillment of the
requirements for the degree of
Master of Science

Nguyen Thi Phuong Thao

01/11/2021

Approved by



Advisor

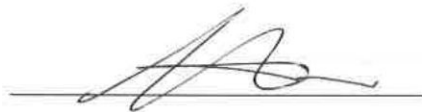
Joo Hun Kang

A porous membrane-integrated PMMA microfluidic
device for reliable cytotoxicity tests.

Nguyen Thi Phuong Thao

This certifies that the thesis/dissertation of Nguyen Thi Phuong Thao is approved.

01/11/2021



Advisor: Joo Hun Kang



Tae-Eun Park: Thesis Committee Member #1



Suk-kyun Ahn: Thesis Committee Member #2

Abstract

High-throughput microfluidic devices for cytotoxicity screening are currently in high demand because they take much less turnaround time and cost only a fraction to fabricate comparing to the traditional animal testing method. However, most of the previous works have failed to construct a reliable drug testing platform since the largely exploited material - polydimethylsiloxane (PDMS) – absorbs even small hydrophobic molecules, such as anti-cancer drugs. Several previous studies have switched to thermoplastics, including poly(methyl methacrylate) (PMMA), for its inherent impermeability to small molecules. Still, there is no record shown to integrate these resins with polyethylene terephthalate (PETE) track-etched membrane to form a fully compartmentalized chip. This study reports a novel use of (3-glycidyloxypropyl)trimethoxysilane (GLYMO) to achieve an irreversible bonding of PMMA to PETE membranes for developing a drug-testing model. Briefly, the PMMA substrates engraved with microfluidic channels were functionalized with air plasma for 1 min and assembled with a 5% GLYMO - coated PETE membrane, followed by clamping and heating in an oven at 100 °C for 2 min. The fabricated device endured up to 135kPa in gauge pressure and $1.97 \times 10^7 \text{ kg m}^{-2}$ in shear force before showing any signs of liquid leakage. Drug testing efficacy was successfully validated as human lung adenocarcinoma cells showed more reliable cytotoxicity results for vincristine when cultured in the PMMA devices than those in the PDMS counterpart. Overall, our bonding approach was proven to be more advantageous over the fabrication methods using PDMS to construct a highly robust and reliable microfluidic device for promising pharmaceutical drug screening applications.

Contents

I.	Introduction-----	11
II.	Materials and method-----	12
	2.1 Microfluidic channel design and fabrication-----	12
	2.2 Chemical bonding strategy-----	14
	2.3 Cell culture-----	16
	2.4 Bonding strength measurement-----	17
	2.5 Small molecule absorption -----	17
	2.6 Cytotoxicity testing of drug-----	18
	Statistical analysis-----	18
III.	Results and discussion -----	19
	3.1 Bonding strategy and experimental validation-----	19
	3.2 Bonding strength evaluation-----	23
	3.3 Cell culture and cytotoxicity testing of drug-----	25
IV.	Conclusion-----	29
V.	Reference -----	30
VI.	Acknowledgment -----	31

List of figures

Figure 1. (A) Schematic diagram of the overall chip assembling process. (B) Microfluidic channels are engraved on the PMMA substrates using a CNC machine. (C) 5% GLYMO-treated PETE membrane is sandwiched between two layers of air plasma-treated PMMA substrates. (D) Tygon tubes are connected to the inlets and outlets of a fully bonded chip for ease of fluid manipulation. Scale bar, 1cm.

Figure 2. A schematic diagram of chemical bonding between PMMA substrates and porous PETE membrane. (A) PETE membrane is first oxidized by air plasma treatment and coated with 5% GLYMO solution. (B) PMMA substrates (both upper and lower layer) are air-plasma treated (C) GLYMO-coated PETE membrane is brought into contact with oxidized PMMA substrates to form an irreversible bonding under thermal catalyst.

Figure 3. Surface characterization of PETE membrane after chemical treatment. (A)-(I) SEM images of the porous PETE membrane when in bare condition, air plasma-treated, and GLYMO-treated. Scale bar, 100 μm (A), (D), (G); 50 μm in (B), (E), (H); 10 μm in (C), (F), (I). Contact angles were also measured (J) for three same conditions.

Figure 4. (A) XPS analysis of the GLYMO - treated PETE membrane. (B) The SiC bond is derived from the GLYMO molecules. (C), (D) The C 1s and O 1s spectra showing multiple peaks represent polyester on the PETE surface. (E) The Si 2s and Si 2p peaks are shown because of the silane coupling reaction.

Figure 5. FT-IR analysis of (A) GLYMO-treated PETE membrane and (B) APTES-treated PETE membrane compared against air-plasma treated PETE membrane, respectively. (C) FT-IR analysis of APTES-treated PMMA substrate versus air plasma-treated PETE membrane.

Figure 6. Validation of robust bonding. (A) The bonding strength between PMMA and PETE membrane was measured in terms of shear stress. GLYMO-coated PETE bonded to hydroxylated PMMA substrates showed the highest resistance to shear force compared to other bonding methods. (B)(C)(D) The fabricated device was confirmed to be leakage-free by using a dye-penetration test.

Figure 7. Diagrammatic top-view representations of the microfluidic channels and PETE membranes assembled with PMMA and PDMS. Scale bars, 400 μm . (A) The flat PETE membrane in the PMMA – PETE device. (B) The irregularly wrinkled PETE membrane in the PDMS – PETE device. (C) Confocal microscopic images (orthogonal section display mode) showing calcein-AM-stained human lung adenocarcinoma cells (green) cultured for 2 days on PETE membrane in the PMMA

and PDMS devices, respectively. The two inset panels at the top and right sides of the images depict the longitudinal and lateral cross-sectional views of the cells cultured on the membrane in the PMMA and PDMS devices, respectively.

Figure 8. Small molecule absorption degree evaluation using dye-penetration test. (A) Rhodamine B solution flowed through the PDMS-PETE and PMMA-PETE channel for 4 to 16 hours. The fluorescence images captured from the top view shows the dye solution absorbed into the substrates at each different time point. Neither PMMA nor PETE absorbed the rhodamine B dye while the PDMS significantly absorbed the dye. The fluorescence intensity of the PETE membrane (bottom panel of A) was measured after washing out the channel with a buffer solution to remove residual rhodamine B dyes in the channel. Scale bar: 200 μm . (B) The quantitative comparison of rhodamine B absorbed into the PDMS channel, the PMMA channel, and the PETE membrane, respectively.

Figure 9. Cytotoxicity testing of Vincristine (at 300nM and 1 μM concentration) on human lung adenocarcinoma cells cultured in PDMS and PMMA devices for 48 hrs.

List of table

Table 1. Summary of chemical bonding strategies. We investigate the bonding of (i) Hydroxylated PMMA (OH-PMMA) to GLYMO-PETE membrane, and for comparison, we also evaluate bonding of (ii) Hydroxylated PMMA (OH-PMMA) to APTES-PETE membrane, (iii) APTES-PMMA to GLYMO-PETE membrane, and (iv) Hydroxylated PDMS (OH-PDMS) to GLYMO-PETE membrane.

1. Introduction

Over the past decades, the development and testing stage of the drug pipeline has been heavily constrained due to the rigorous regulation and expensive production cost, resulting in very few medicines making to the market each year¹. This burden is only worsened due to the upsurge of drug discovery services. According to a recent report, its market size is forecasted to expand exponentially, reaching an estimated value of up to USD 21.4 billion in 2025². Despite many efforts toward outsourcing analytical testing and clinical trials, keeping up with such enormous demand remains extremely challenging to this day.

A potential solution to overcome this difficulty would be screening drugs through a lab-on-a-chip platform. Owing to their miniaturized scale, the microfluidic devices allow manipulation of small sample volume with precise control, making them an excellent choice for throughput chemical and biological assays³. Many have attempted to construct drug testing models using microfluidic approaches and obtained certain successes. For example, Bo et al. aligned quartz substrate-embedded microwell array containing sol-gel bioreactor with a cell culture chamber to achieve a compact drug metabolite profiling system. Acetaminophen (AP) was introduced into the device and the corresponding viability of human liver cancer cells (HepG2) on the bottom channel was then collected and analyzed⁴. Jatz et al. utilized a gradient generator complex to expose mouse embryo cells (Balb/c 3T3) and human lung carcinoma cells (A549) to various concentrations of celecoxib (Celbx)/ 5-fluorouracil (5-FU) for as long as 48 hrs⁵. Although instrumental in analyzing the toxic effect of drugs, most of these testing models are unreliable because of the device materials. Among many others, poly(dimethylsiloxane) (PDMS) is the most extensively used polymer for prototyping microfluidic chips because of the benefits it offers such as facile sealing and optical transparency⁶. However, PDMS substrates are prone to absorb small hydrophobic molecules like anti-cancer drugs, so partitioning of molecules into PDMS chip can significantly change solution concentrations and could potentially alter experimental outcomes⁷.

To this end, many researchers have employed thermoplastic materials such as polymethylmethacrylate (PMMA), polycarbonate (PC), cyclic olefin copolymer (COC) as an alternative to conventional silicon or glass material. These resins present rigid mechanical property, high compatibility to electrophoresis, and strong resistance to chemicals and solvents⁸, which thereby make them a better fit for cytotoxicity testing of drugs, compared to the PDMS-based microfluidic setting.

To construct a fully compartmentalized microfluidic device from thermoplastic resin, several bonding methods were previously explored. These include thermal bonding⁹, thermal fusion¹⁰, microwave bonding¹¹, adhesive bonding¹², and solvent bonding¹³, etc. Although thermal bonding is the most widely

used method, high temperature and pressure often can distort the geometry of the micro-scaled channels. On the other hand, solvent-assisted thermal bonding enables the reservation of channel structure as the bonding occurs at a much lower temperature. This is because the chemical linker acts as a plasticizer to reduce glass transition temperature on the surface of the thermoplastic. Still, previous studies mostly focused on exploiting chemical reagent like (3-aminopropyl)triethoxysilane APTES, (3-glycidyoxypropyl) trimethoxysilane (GLYMO), to achieve an irreversible bonding between thermoplastic substrates, but not between the substrate to porous polyethylene terephthalate (PETE) track-etched membrane, which is crucial for exchange of cellular signals between chambers.

To address these unmet challenges, we developed a simple bonding method of PMMA to porous PETE membrane using coupling reagent GLYMO for a compartmentalized drug testing model. We further validated our model's efficacy by obtaining the viability of human lung cancer cells when exposed to the anti-cancer drug vincristine. Our proposed method is promising in lowering the entry barrier for prototyping microfluidic chips for cytotoxicity tests of drugs.

2. Materials and method

2.1 Microfluidic channel design and fabrication

Microfluidic channel dimensions (width \times height \times length ; 800 μm \times 300 μm \times 800 μm) were outlined in computer-aided design software AutoCAD and encoded before being directly engraved on PMMA substrates (width \times height \times thickness; 5 cm \times 10 cm \times 2 mm) using computer numerical control (CNC) machine (David 3020C, David, Incheon, South Korea). The resulting micropatterns include one cell-culture channel on the lower layer; two through-hole inlets ($D = 1.58$ mm), two through-hole outlets ($D = 1.58$ mm), and a single cell culture channel on the upper channel. The engraved PMMA substrates were then washed with isopropanol (IPA, Samchun Pure Chemical, Gyeonggido, South Korea), deionized (DI) water, and dried with pressurized nitrogen gas. To remove any remaining milling marks, we added 2.5 μL of ethanol (94%) on the microfluidic channels and flipped the PMMA upside down before placing it on a glass slide inside a convection oven (C-D0D1, Changshin Science, Gyeonggido, South Korea) at 100°C for 2 minutes. Since sudden temperature change may result in a crack inside the device's channels, the PMMA substrates are stored in a convection oven at 60°C for around 20 mins before the chemical bonding step.

A

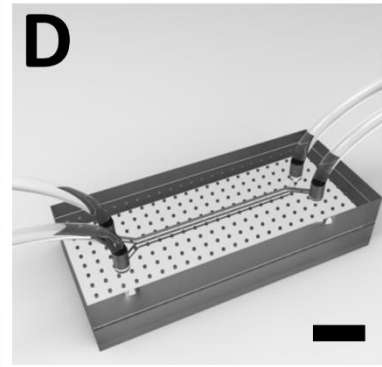
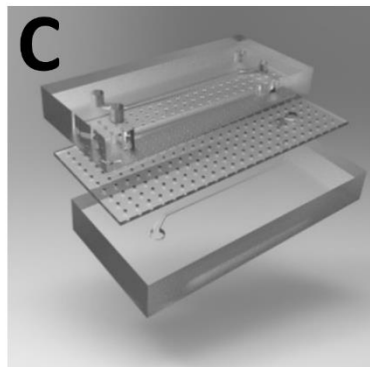
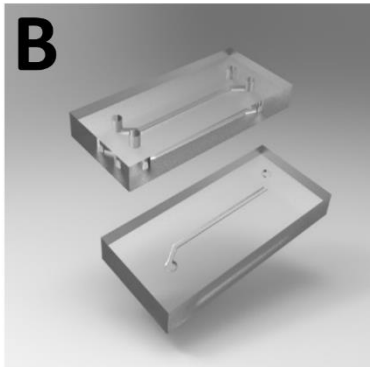
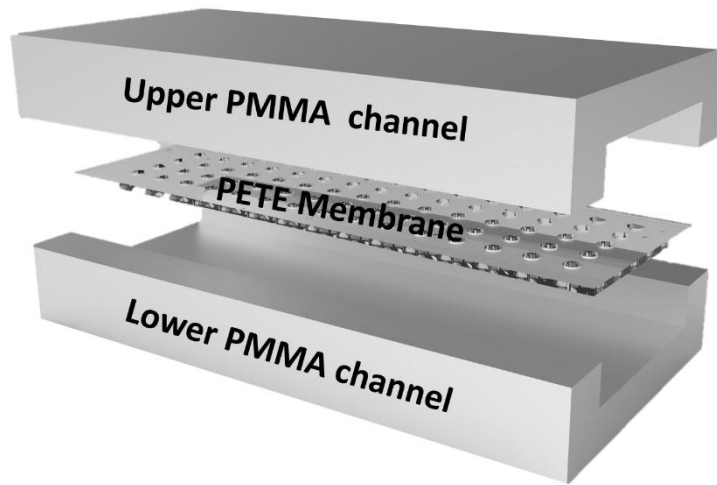


Figure 1. (A) Schematic diagram of the overall chip assembling process. (B) Microfluidic channels are engraved on the PMMA substrates using CNC machine. (C) 5% GLYMO-treated PETE membrane is sandwiched between two layers of air plasma-treated PMMA substrates. (D) Tygon tubes are connected to the inlets and outlets of a fully bonded chip for ease of fluid manipulation. Scale bar, 1cm.

2.2 Chemical bonding strategy

Hydrophobic track-etched PETE membrane (1 μm pore size, SterliTech, Kent, WA, USA) was trimmed to fit the PMMA substrates (width x length; 3.5 cm x 3.5 cm) and subsequently rinsed with IPA, DI water before gently blow-dried with pressurized nitrogen gas. PETE membrane was oxidized with air plasma treatment (80 W, 50 kHz Cute-1MPR, Femto Science, Gyeonggido, South Korea) for 1 min, so the surface was rendered hydrophilic. It was then further modified chemically by being immersed in GLYMO solution (5 wt%, dissolved in ethanol (99%), Sigma-Aldrich, MO, USA). The chemical flask was placed on a hot plate at 100°C for 40 mins. In the meantime, previously machined PMMA substrates (upper and lower layer) were cooled to room temperature for 5 mins and oxidized via air plasma (80 W, 50 kHz) for 1 min. To assemble a complete device, we sandwiched a GLYMO-soaked PETE membrane in between the upper and lower PMMA layer and secured with paper clamps on sides after confirming the channels' borders were well aligned under an LCD digital microscope (1-600X, Junefor, China). The whole device was placed inside a convection oven at 100°C for 2 mins. Under thermal catalyst, hydroxyl groups generated on the surfaces of PMMA substrates would couple with epoxide groups from GLYMO coated PETE membrane to form an irreversible bonding. The bonded device was let dried in a convection oven at 60 °C for no more than 24 hrs and finally stored at room temperature until the next use. Tygon tubes (ID 0.508 mm \times OD 1.524 mm, Saint-Gobain PPL Corp., USA) were glued to the inlets and outlets using 5-minute epoxy glue (Loctite, OH, USA) for further flow manipulation inside the microfluidic device (Fig.2). In addition to this, we also compared other chemical functionalization techniques (ii, APTES-PETE to OH-PMMA and iii, GLYMO-PETE to APTES-PMMA) and alternative substrates to PMMA, such as PDMS (iv, GLYMO-PETE to OH-PDMS) to prove the superiority of the proposed method (Table 1). The topological integrity of the PETE membrane surface was assessed post-treatment using Scanning electron microscopy (SEM) images (S4800, Hitachi High Technologies, USA). Chemical composition was evaluated using X-ray photoelectron spectroscopy (XPS, K-alpha, Thermo Fisher, Seoul, South Korea) and FT-IR spectroscopy (Cary 670-IR FT-IR Air-Bearing Spectrometer, Agilent Technologies, CA, USA) while contact angle was estimated using contact angle measurements (Phoenix 300, SEO – Surface Electro-Optics, Gyeonggido, South Korea) (Fig. 3).

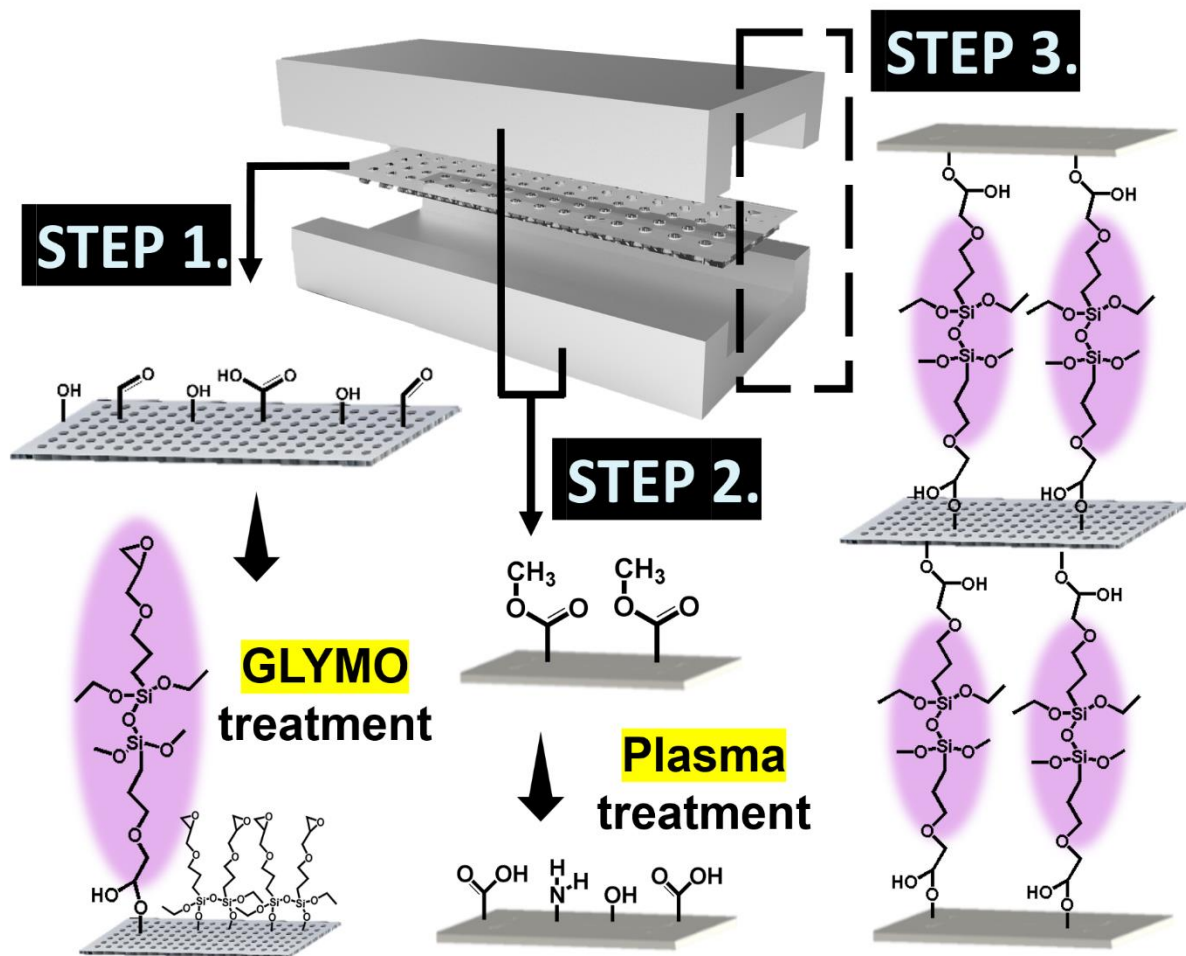


Figure 2. A schematic diagram of chemical bonding between PMMA substrates and porous PETE membrane. (A) PETE membrane is first oxidized by air plasma treatment and coated with 5% GLYMO solution. (B) PMMA substrates (both upper and lower layer) are air-plasma treated (C) GLYMO-coated PETE membrane is brought into contact with oxidized PMMA substrates to form an irreversible bonding under thermal catalyst.

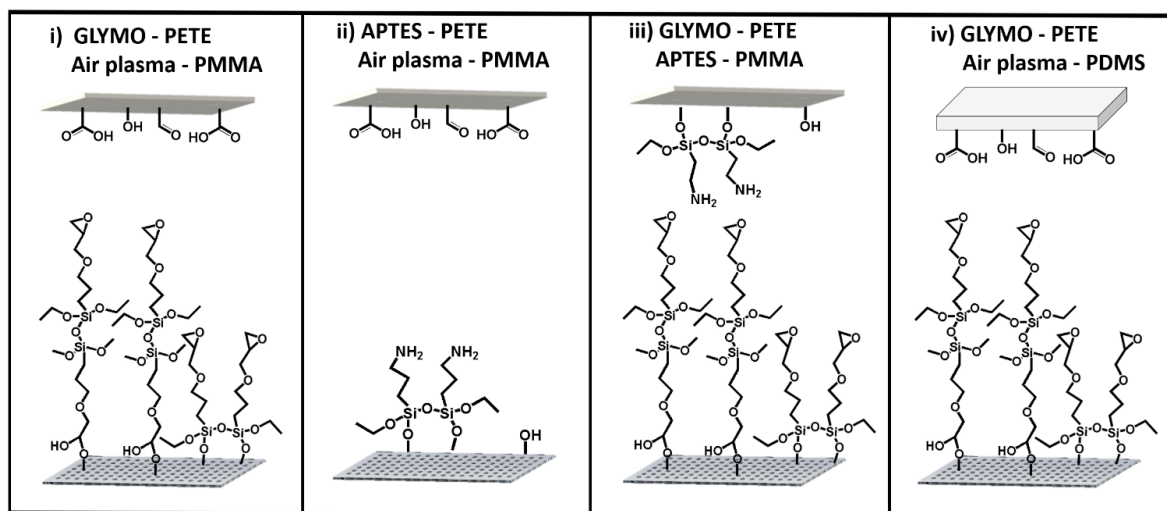


Table 1. Summary of chemical bonding strategies. We investigate the bonding of (i) Hydroxylated PMMA (OH-PMMA) to GLYMO-PETE membrane, and for comparison, we also evaluate bonding of (ii) Hydroxylated PMMA (OH-PMMA) to APTES-PETE membrane, (iii) APTES-PMMA to GLYMO-PETE membrane, and (iv) Hydroxylated PDMS (OH-PDMS) to GLYMO-PETE membrane.

2.3 Cell culture

For sterilization, the microfluidic channels were flushed with ethanol (70%) thoroughly three times to eliminate any remaining chemical residues post-treatment. The channels were sequentially rinsed with phosphate-buffered saline (PBS) and cell culture medium. Ham's F12 medium (supplemented with 10% fetal bovine serum and 1% penicillin-streptomycin, Welgene, Gyeongsangbuk-do, South Korea) was used when culturing human lung adenocarcinoma cells (A549, ATCC® CCL-185™) and endothelial cell medium (supplemented with 10% fetal bovine serum and 1% penicillin-streptomycin, Sciencell, CA, USA) was used when culturing primary human umbilical vein endothelial cells (HUVEC) (Lonza, Switzerland). To further enhance the cell adhesion, the channels were coated with fibronectin (15 $\mu\text{L mL}^{-1}$ in PBS) and collagen (20 $\mu\text{L mL}^{-1}$ in PBS) in an incubator (37 °C, 5% CO₂ gas) for 1 hr, respectively. Cancer cells (A549) and primary cells (HUVEC) were chosen to prove the versatility and compatibility of our fabricated microfluidic device with different cell types. When reached 70% confluency, cells were washed with PBS, trypsinized, and the centrifuged cell pellet was resuspended into media at 1.0 x 10⁶ cells per mL concentration. The cell solution was gently loaded through the

Typgon tube connected at the inlet port and manually pumped through the bottom channel until the solution reaches the outlet. The microfluidic device was inverted and kept inside an incubator for 2 hrs to allow cell attachment on the upper PETE membrane layer. After confirming that cells are firmly seeded, media was flowed through both channels at a flowrate of $2 \mu\text{L min}^{-1}$ using a syringe pump (Fusion 200, Chemyx Inc., USA). For cell visualization, we added calcein acetoxymethyl ester (calcein-AM) solution ($2 \mu\text{M}$ in PBS) to the bottom channel and incubated at room temperature for 40 minutes, then observed using a confocal microscope (LSM 780 Configuration 16 NLO; Carl Zeiss, USA). Optical slicing along the z -axis was carried out to recreate the cell monolayer cultured on PETE membrane and obtain their spatial distribution in 3D.

2.4 Bonding strength measurement

The integrity and stability of the bonding between PMMA and PETE membrane were evaluated using uniform transmembrane pressure (UTP) shear test (4000 Plus Bondtester, Nordson Dage, OH, USA) (shear height: $20 \mu\text{m}$, test speed: $500 \mu\text{m s}^{-1}$, maximum cartridge weight: 200 kg). The bonded microfluidic chip was fitted tightly into the sample holder and cartridge weight was increased over time until the upper PMMA layer slid off the PETE membrane while the lower PMMA layer remained attached to the porous membrane (Fig.3). The shear stress was obtained by dividing the failed loading weight by the bonding area (width x length; $3.5 \text{ cm} \times 3.5 \text{ cm}$). For comparison, we also evaluated other bonding strategies as shown in Table 1, where (i) hydroxylated PMMA (OH-PMMA) was bonded to APTES-PETE membrane and (iii) APTES-PMMA was bonded to GLYMO-PETE membrane. The test was performed for at least 3 trials per sample and conducted inside a specialized laboratory to eliminate the nuanced change in temperature, moisture, or contact with any solvents or fluids that might influence the result. For the leakage test, we filled the chip with color-dyed solutions (red and green) through each upper and lower microfluidic channel, and progressively increasing the inlet pressure every 20 seconds with a constantly closed outlet. The maximum internal pressure was recorded before the liquid burst outside of the channel using a pressure sensor (Harvard Apparatus, USA).

2.5 Small molecule absorption

To determine the small molecule absorption by PDMS or PMMA substrates, dye-penetration testing was performed. In detail, rhodamine B (1mM) solution was flowed continuously through both microfluidic channels, at a flow rate of $2 \mu\text{L}/\text{min}$ for 16 hrs. Fluorescence images were obtained every hour and analyzed in ImageJ program.

2.6 Cytotoxicity testing of drug

Vincristine was chosen for the cytotoxicity testing because of its extensive use in treating several cancer. To prepare the drug solution, Vincristine (Sigma-Aldrich, USA) was dissolved in distilled water to a concentration of 5 mM. It was further diluted in the culture medium to achieve a concentration of 300 nM and 1 μ M. Prepared drug solution then flowed through the lower channel of the microfluidic device at a flow rate of 25 μ L/hr for 48 hrs. After drug treatment, cells were stained with fluorescence dyes for viability assessment, specifically live cells were labeled with Hoechst (Sigma-Aldrich, USA) while dead cells were labeled with propidium iodide (PI) (Sigma-Aldrich, USA). The recommended concentration from the live/dead kit (Sigma-Aldrich, USA) was followed, where 1 μ g/ml of PI and 0.5 μ g/ml of Hoechst was added to the culture medium and infused into the cell channel for 40 mins at room temperature. Before fluorescent imaging, PBS rinsing and paraformaldehyde (PFA) fixation was each performed for 15 mins before fixating the cells. At least three random spots within the microfluidic channel were chosen and images were captured at 10 \times magnification was using a confocal microscope (LSM 780 Configuration 16 NLO). The images were analyzed using an image processing software (Imaris, Bitplane; <http://www.bitplane.com>) and then calculated using equation (1).

$$\text{Viability} = \frac{\sum_{\text{optical sections}} \left[\frac{\text{No. of blue objects} - \text{No. of red objects}}{\text{No. of blue objects}} \right]}{\text{No. of optical sections}} \times 100 \% \quad (1)$$

Statistical analysis

The results are presented as an average of at least triplicate samples \pm standard error means depicted by error bars in all of the graphs. Significant differences in all data were determined using the two-tailed Student's *t*-test, as defined by *P* values < 0.05.

3. Result and discussion

3.1 Bonding strategy and experimental validation

Air plasma treatment is often used as a means of adding biological relevant functional groups like hydroxyl groups (-OH) or other oxygen-containing groups (e.g., -(C=O)H, -(C=O)OH, etc.) to material surfaces. As a result, plasma-treated surfaces such as PETE and PMMA become more readily available to react when brought into contact with other substrates. GLYMO is widely employed as a coupling agent or an adhesion promoter because a terminal epoxide group is reactive toward common nucleophiles, including -NH₂, -OH, and -SH, while the trimethoxy silane group can readily form C-O-Si bonds by reacting with -OH of polymers through hydrolysis, followed by condensation. Considering the aforementioned characteristics, we decided to use GLYMO as an adhesive to covalently link between i) the GLYMO-functionalized PETE membrane (GLYMO-PETE) and the hydroxyl-functionalized PMMA (OH-PMMA). In addition, we also treated ii) the PETE membranes with APTES (APTES-PETE) to compare the bonding strength with the GLYMO-treated PETE membranes, and predicted that the bonding of GLYMO-PETE to OH-PMMA would be much stronger than APTES-PETE to OH-PMMA. This prediction can be attributed to the fact that the hydroxyl groups on plasma-treated PMMA have higher reactivity toward the epoxide groups on GLYMO-PETE than to the amine groups from APTES-PETE. Finally, we also attempted to bond iii) the GLYMO treated PETE membranes (GLYMO-PETE) to the APTES-functionalized PMMA substrates (APTES-PMMA) because amine groups in APTES are known to be reactive with epoxide groups in GLYMO.

In order to validate our bonding strategy between the PETE membranes and the PMMA substrates, we first characterized the surface functionalization by obtaining SEM images, contact angles, and XPS measurement of the membrane when in bare form, air plasma-treated and GLYMO-treated. SEM images confirmed that the porous structures of the track-etched PETE membranes were completely retained even after GLYMO treatment and heating at 100 °C for 2 min (Fig. 3). The water contact angles measured on the bare PETE membrane surface, the air-plasma treated surface, and the 5% GLYMO treated surface were $98.443^\circ \pm 0.651^\circ$, $46.146^\circ \pm 1.342^\circ$, and $82.911^\circ \pm 1.004^\circ$, respectively (Fig. 4). This indicates the topography change after plasma and chemical treatment where the plasma-treated surface became more hydrophilic and after coated with GLYMO, it became more hydrophobic but not as much as in the bare form. The siloxane groups (Si2s and Si2p) shown in the XPS spectra supported the successful functionalization of GLYMO on the PETE surface (Fig. 5). For more quantitative analysis of the surface functionalization, we assessed the inherent density of the elements on the PETE and PMMA surfaces using FT-IR analysis. The higher peak intensity in the FT-IR spectra represents the

higher density of a functional group associated with a certain molecular bond. It is noticeable that there was a drastic increase in the proportion of C-H, C=O, C-O bonds in i) the GLYMO-treated membranes in comparison to ii) the APTES-treated PETE membranes (Fig.6). In addition, iii) the PMMA substrates treated with APTES (APTES-PMMA) yielded a lower peak intensity than the air-plasma treated PMMA substrates (OH-PMMA), which implies that the number of amine groups formed on the PMMA surface is smaller than that of hydroxyl groups on the surface driven by air plasma treatment. Hence, as more epoxide groups on the GLYMO-treated PETE membrane were available for bonding with hydroxyl groups on the PMMA substrates, we predicted that the stronger bond strength would be achieved between the GLYMO-PETE membranes and the air plasma-treated PMMA substrates (OH-PMMA).

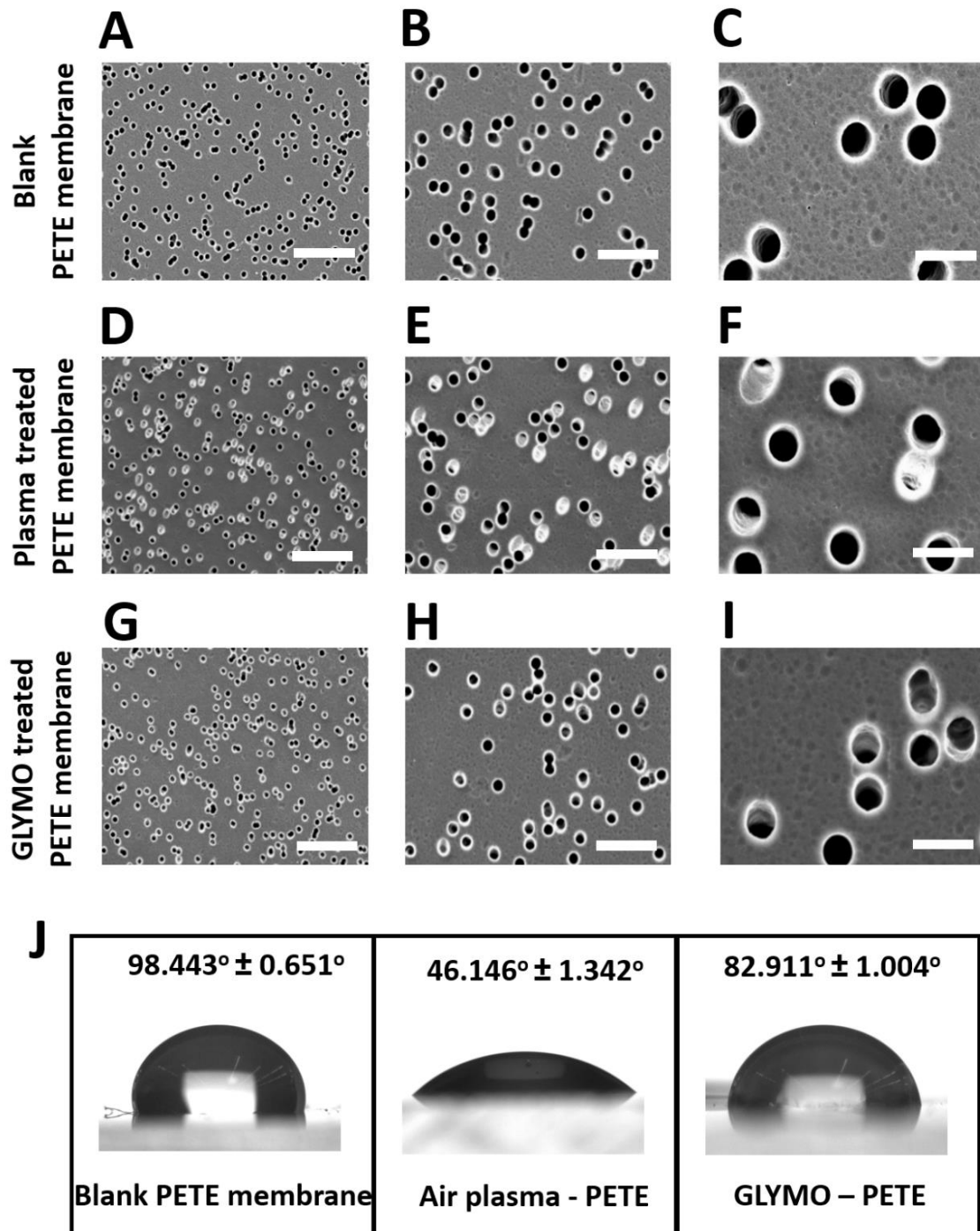


Figure 3. Surface characterization of PETE membrane after chemical treatment. (A)-(I) SEM images of the porous PETE membrane when in bare condition, air plasma-treated, and GLYMO-treated. Scale bar, 100 μm (A), (D), (G); 50 μm in (B), (E), (H); 10 μm in (C), (F), (I). Contact angles were also measured (J) for three same conditions.

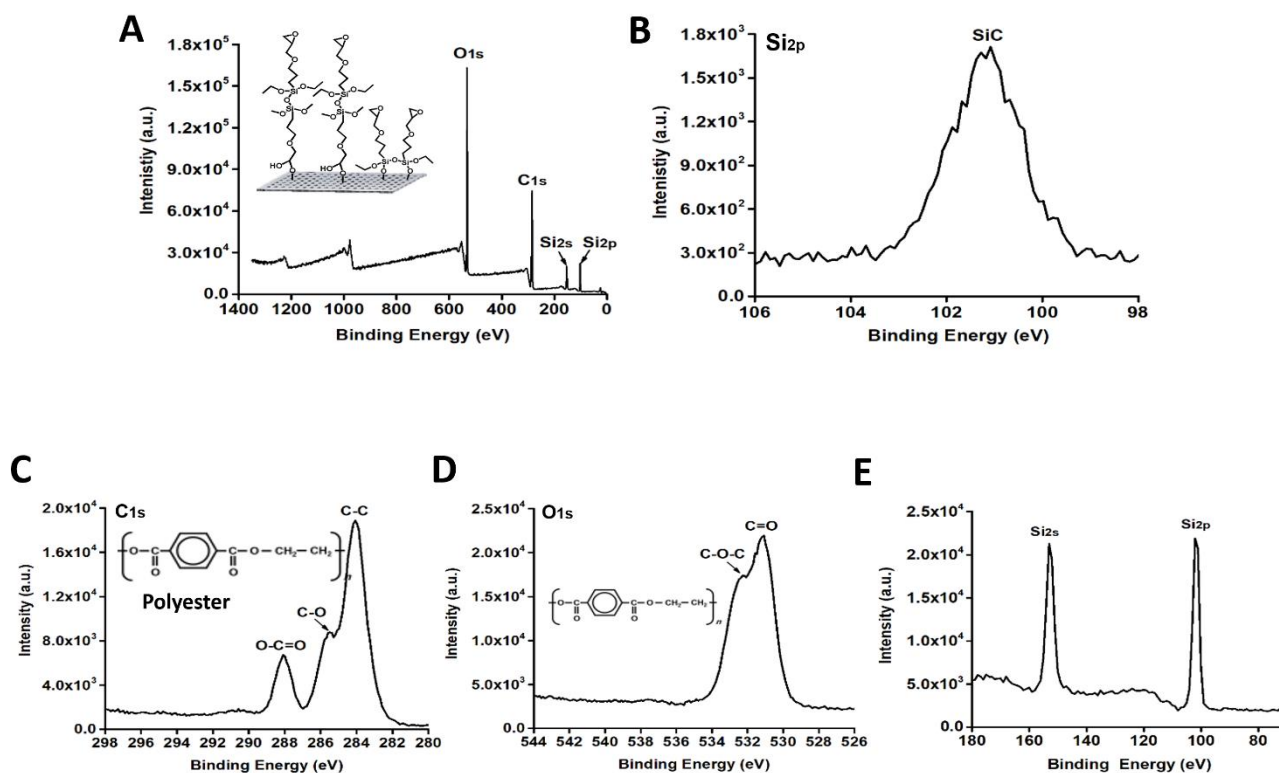


Figure 4. (A) XPS analysis of the GLYMO - treated PETE membrane. (B) The Si1s bond is derived from the GLYMO molecules. (C), (D) The C 1s and O 1s spectra showing multiple peaks represent polyester on the PETE surface. (E) The Si 2s and Si 2p peaks are shown because of the silane coupling reaction.

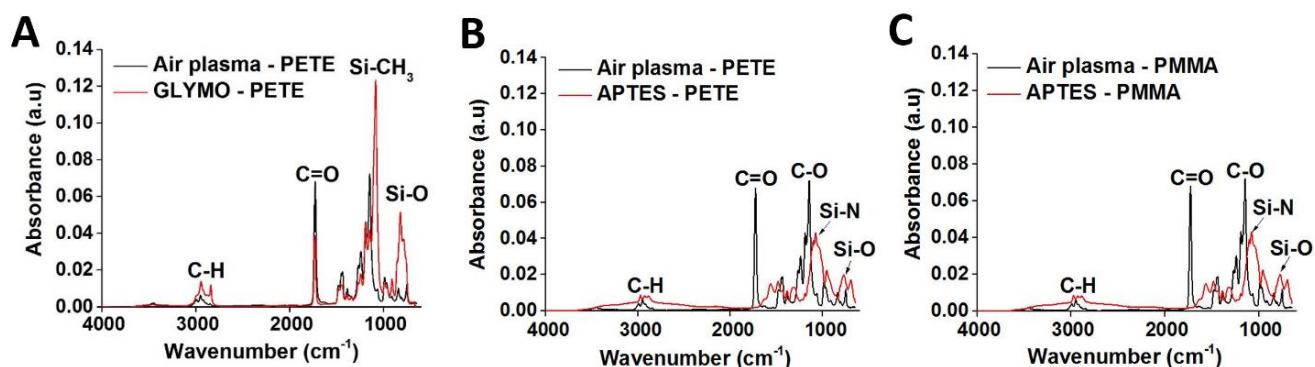


Figure 5. FT-IR analysis of (A) GLYMO-treated PETE membrane and (B) APTES-treated PETE membrane compared against air-plasma treated PETE membrane, respectively. (C) FT-IR analysis of APTES-treated PMMA substrate versus air plasma-treated PETE membrane.

3.2 Bonding strength evaluation

We compared the bonding strength between the PETE membranes and the PMMA substrates, achieved by various chemical bonding strategies including i) GLYMO-PETE to OH-PMMA, ii) APTES-PETE to OH-PMMA, and iii) GLYMO-PETE to APTES-PMMA. As shown in Fig. 6, the shear stress endured by i) GLYMO-PETE to OH-PMMA was around $1.97 \times 10^7 \text{ kg/m}^2$, which is much greater than the other two experimental conditions (ii, APTES-PETE to OH-PMMA: $1.33 \times 10^7 \text{ kg/m}^2$ and iii, GLYMO-PETE to APTES-PMMA: $1.14 \times 10^7 \text{ kg/m}^2$). As we predicted, the bonding between GLYMO-PETE and OH-PMMA provided a stronger and more robust bonding than the other cases. This higher reactivity is presumably due to the higher bioreactivity of the hydroxyl group (-OH) of the PMMA substrates to an epoxide group in GLYMO than when reacting to the amine group (-NH₂) from APTES coated on PETE membrane. However, contradicting our prediction, the bonding strength between GLYMO-PETE to APTES-PMMA was not as high as that of GLYMO-PETE to OH-PMMA because of the density of amine groups formed on the PMMA substrate was much lower than hydroxyl groups on the air-plasma treated PMMA substrates. We tested various concentrations of GLYMO and APTES to functionalize the surface in a range of 1 ~ 5 %, treating the PETE surface with 5% GLYMO resulted in the strongest bonding with the PMMA substrates (Data not shown). In addition, we validate the robust bonding by conducting a leakage test. We flowed the color-dyed solution through the microfluidic channel and increase the internal pressure gradually all while clamping the Tygon tube at the outlets. The device could endure up to above 135 kPa of gauge pressure (the upper limit of the pressure sensor) without

any bursts. No leakage was found in the device even when we continuously flowed the solution for four weeks and the success rate of the device fabrication was higher than 99%.

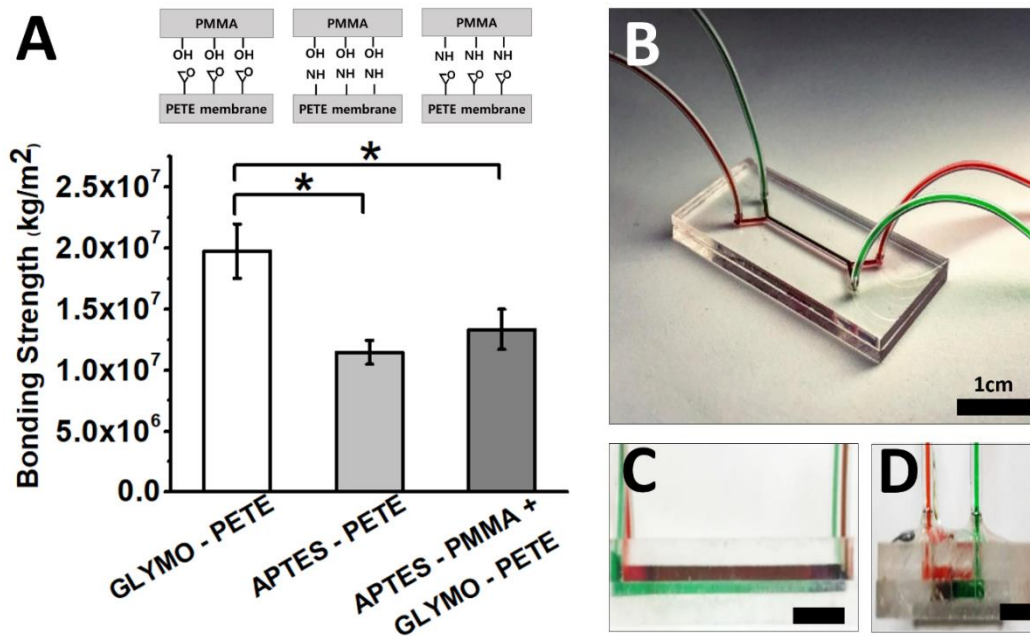


Figure 6. Validation of robust bonding. (A) Bonding strength between PMMA and PETE membrane was measured in term of shear stress. GLYMO-coated PETE bonded to hydroxylated PMMA substrates showed the highest resistance to shear force compared to other bonding methods. (B)(C)(D) The fabricated device were confirmed to be leakage-free by using dye solution.

3.3 Cell culture and cytotoxicity testing of drug

To test the compatibility of the PMMA or PDMS devices with cell culture, we seeded human lung adenocarcinoma cells on the track-etched PETE porous membranes incorporated inside the microfluidic devices and allowed them to proliferate up to 7 days. While the PMMA device showed a clear and flat PETE membrane surface, the membranes integrated into the PDMS device were found wrinkled and warped, which is most likely due to the difference in the thermal expansion coefficient between the PETE membrane and the PDMS substrates (Fig. 7 A, B). This uneven membrane surface could hinder the imaging process. As shown in Fig. 7 C (left), cancer cells (A549) were well seeded inside the PMMA chip and easily recognized under a microscope whereas the entire cell images in the PDMS chip cannot be acquired at a certain focal plane due to the irregularly deformed membrane structures. Primary cells (HUVEC) were also seeded and similar difficulty was encountered (data not shown). Moreover, the irregular surface area of the membranes could significantly affect analytical outcomes because most cell toxicity and membrane permeability are often normalized to the surface area of the membranes. The difference between PMMA and PDMS chip was also apparent in terms of small molecule absorption. When a dye-penetration test was conducted and hourly fluorescent pictures were taken, PDMS was shown to absorb much more dye at 4 hr time point compared to how much PMMA substrates absorb at 16 hr (Fig. 8). Hence, we predicted that there would be a similar result in the cytotoxicity test with drugs.

We observed the cytotoxicity response of human lung adenocarcinoma cells to an anticancer drug (vincristine) after 48 hr of treatment in the PMMA and PDMS devices. The cytotoxicity of the cells cultured in the PMMA and PDMS devices showed a significant difference ($P < 0.05$) when they were treated with 300 nM of vincristine as shown in Fig. 9 (the cell viability of $99.51 \pm 0.27\%$ and $85.43 \pm 2.25\%$, respectively). This can be explained as a considerable amount of vincristine has been absorbed into PDMS due to the intrinsic hydrophobic molecular characteristics ($\text{LogP} = 2.82$), which, in turn, resulted in a reduction of the drug concentration below 300 nM in the culture medium, and thus increased the cell viability of the cells treated in the PDMS device. Interestingly, when the cells were treated with a relatively higher concentration (1 μM), the difference in the cytotoxicity between the PMMA and PDMS devices became insignificant (Fig. 9). This is because the amount of vincristine absorbed into PDMS becomes negligible in a relatively higher drug concentration. The critical concentration for cells cultured in the PDMS device to be affected by the drug was not calculated since it is dependent on chip design and surface area. In addition, we also tested the cytotoxicity of vincristine in the PDMS devices, which were made by PDMS prepared with various ratios of PDMS precursors and a curing reagent (5:1, 10:1, 20:1); however, these were not apparent to a degree of reduction in the drug concentrations (data not shown). Given the results we obtained above, the material property of the

microfluidic cytotoxicity devices, including the thermal expansion coefficient and drug absorption, would be of significant concern when we have to discriminate subtle differences in drug toxicity at relatively low concentrations in the device.

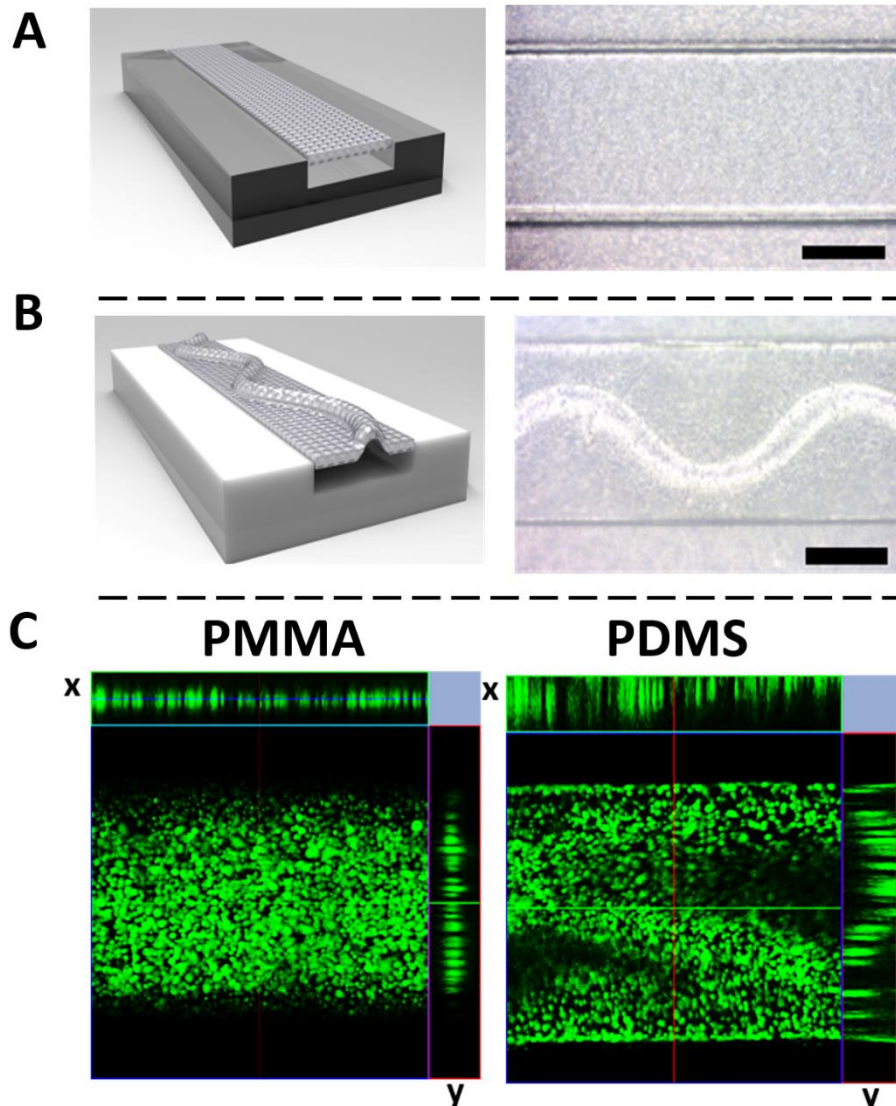


Figure 7. Diagrammatic top-view representations of the microfluidic channels and PETE membranes assembled with PMMA and PDMS. Scale bars, 400 μm . (A) The flat PETE membrane in the PMMA – PETE device. (B) The irregularly wrinkled PETE membrane in the PDMS – PETE device. (C) Confocal microscopic images (orthogonal section display mode) showing calcein-AM-stained human lung adenocarcinoma cells (green) cultured for 2 days on PETE membrane in the PMMA and PDMS devices, respectively. The two inset panels at the top and right sides of the images depict the longitudinal and lateral cross-sectional views of the cells cultured on the membrane in the PMMA and PDMS devices, respectively.

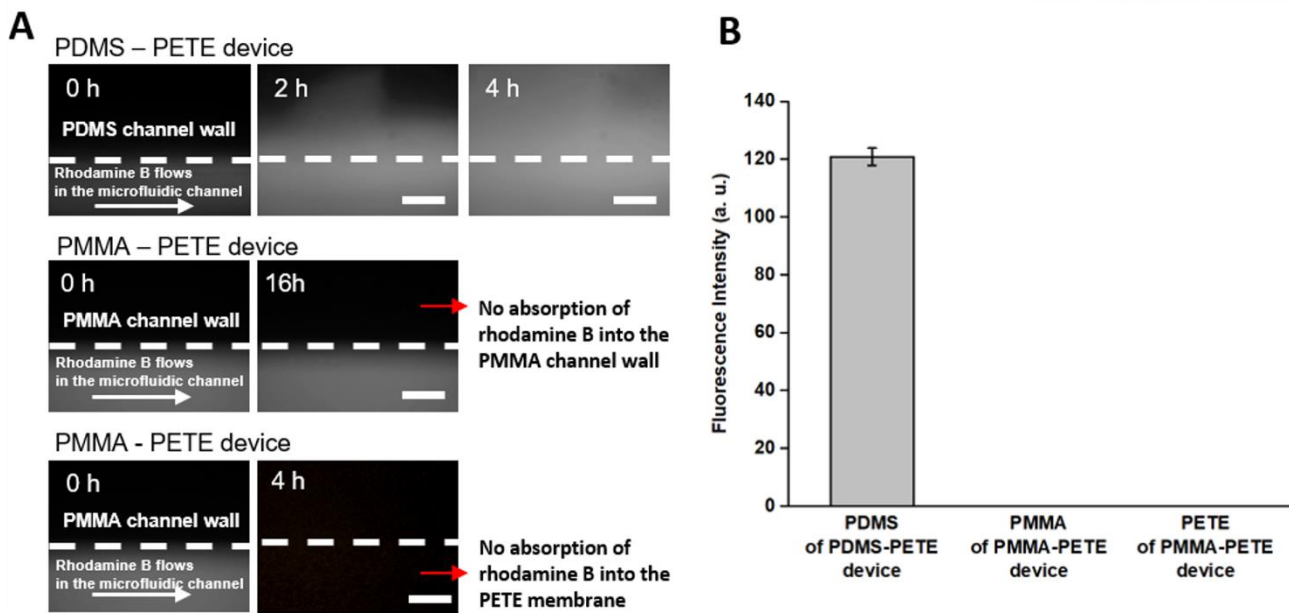


Figure 8. Small molecule absorption degree evaluation using dye-penetration test. (A) Rhodamine B solution was flowed through the PDMS-PETE and PMMA-PETE channel for 4 to 16 hours. The fluorescence images captured from the top view shows dye solution absorbed into the substrates at each different time point. Neither PMMA nor PETE absorbed the rhodamine B dye while the PDMS significantly absorbed the dye. The fluorescence intensity of the PETE membrane (bottom panel of A) was measured after washing out the channel with a buffer solution to remove residual rhodamine B dyes in the channel. Scale bar: 200 μm . (B) The quantitative comparison of rhodamine B absorbed into the PDMS channel, the PMMA channel, and the PETE membrane, respectively.

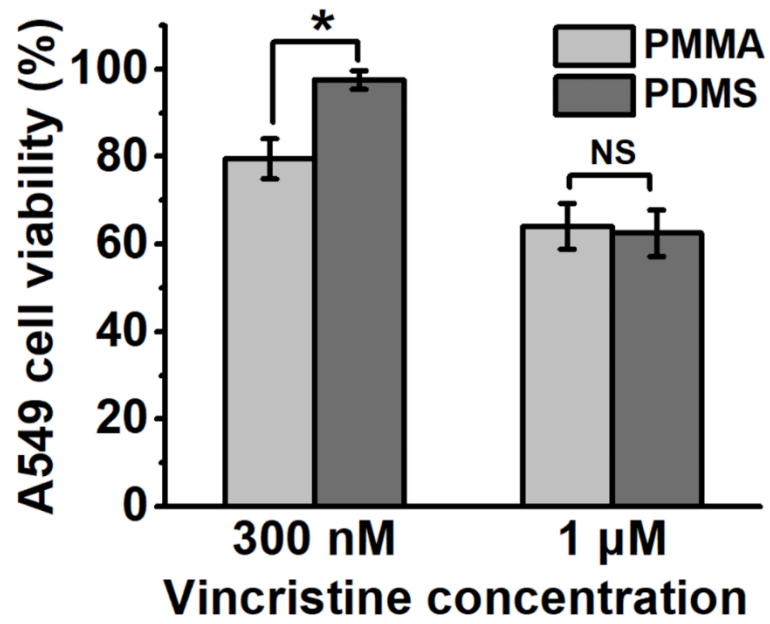


Figure 9. Cytotoxicity testing of Vincristine (at 300nM and 1 μM concentration) on human lung adenocarcinoma cells cultured in PDMS and PMMA devices for 48 hrs.

Conclusion

In this work, we proposed a method to chemically bond PMMA substrates to porous PETE track-etched membranes to achieve a robust microfluidic device for cytotoxicity tests of anticancer drugs. The PETE membrane-integrated PMMA devices enabled a flat and uniform porous membrane and reliable delivery of drugs at a targeted concentration to the cells. We demonstrated that GLYMO-PETE bonded with OH-PMMA yield the strongest bonding strength compared to other chemical bonding strategies, including conventional coupling reagent APTES. We could further explore potential pairs of chemical reagents that allow to bond different polymer or inorganic substrates to fabricate the microfluidic devices that permit various capabilities. To extent usability of organ-on-a-chip or lab on a chip for more practical applications, we believe that our method will provide the great capability to researchers in the field to explore cell and tissue engineering in various conditions more precisely mimicking the micro-physiological environment in vivo.

Reference

1. Matteelli, A. *et al.* Multidrug-resistant and extensively drug-resistant Mycobacterium tuberculosis: Epidemiology and control. *Expert Rev. Anti. Infect. Ther.* **5**, 857–871 (2007).
2. Linker, R. The Drug discovery market. [https://www.globenewswire.com/news-release/2020/09/16/2094263/0/en/The-drug-discovery-services-market-is-projected-to-reach-USD-21-4-billion-by-2025-from-USD-11-1-billion-in-2020-at-a-CAGR-of-14-0.html#:~:text=Filings Media Partners-,The drug discovery services market is projected to reach USD,at a CAGR of 14.0%25 \(2020\).](https://www.globenewswire.com/news-release/2020/09/16/2094263/0/en/The-drug-discovery-services-market-is-projected-to-reach-USD-21-4-billion-by-2025-from-USD-11-1-billion-in-2020-at-a-CAGR-of-14-0.html#:~:text=Filings Media Partners-,The drug discovery services market is projected to reach USD,at a CAGR of 14.0%25 (2020).)
3. Streets, A. M. & Huang, Y. Chip in a lab: Microfluidics for next generation life science research. *Biomicrofluidics* **7**, (2013).
4. Ma, B., Zhang, G., Qin, J. & Lin, B. Characterization of drug metabolites and cytotoxicity assay simultaneously using an integrated microfluidic device. *Lab Chip* **9**, 232–238 (2009).
5. Jastrzebska, E. *et al.* A microfluidic system to study the cytotoxic effect of drugs: The combined effect of celecoxib and 5-fluorouracil on normal and cancer cells. *Microchim. Acta* **180**, 895–901 (2013).
6. Mata, A., Fleischman, A. J. & Roy, S. Characterization of Polydimethylsiloxane (PDMS) Properties for Biomedical Micro/Nanosystems. *Biomed. Microdevices* **7**, 281–293 (2005).
7. Toepke, M. W. & Beebe, D. J. PDMS absorption of small molecules and consequences in microfluidic applications. 1484–1486 (2006) doi:10.1039/b612140c.
8. Ali, U., Karim, K. J. B. A. & Buang, N. A. A Review of the Properties and Applications of Poly (Methyl Methacrylate) (PMMA). *Polym. Rev.* **55**, 678–705 (2015).
9. Zhu, X., Liu, G., Guo, Y. & Tian, Y. Study of PMMA thermal bonding. *Microsyst. Technol.* **13**, 403–407 (2007).
10. Song, I. H. & Park, T. PMMA solution assisted room temperature bonding for PMMA-PC hybrid devices. *Micromachines* **8**, 1–6 (2017).
11. Yussuf, A. A., Sbarski, I., Hayes, J. P., Solomon, M. & Tran, N. Microwave welding of polymeric-microfluidic devices. *J. Micromechanics Microengineering* **15**, 1692–1699 (2005).
12. Dang, F. *et al.* Replica multichannel polymer chips with a network of sacrificial channels sealed by adhesive printing method. *Lab Chip* **5**, 472–478 (2005).
13. Bamshad, A., Nikfarjam, A. & Khaleghi, H. A new simple and fast thermally-solvent assisted method to bond PMMA-PMMA in micro-fluidics devices. *J. Micromechanics Microengineering* **26**, (2016).

Acknowledgment

Throughout the master's degree program, I have received a great deal of support and assistance.

First of all, I would like to express my gratitude to my supervisor, Professor Kang Joo Hun for his kind guidance and constant supervision ever since I started my internship in TMB lab in 2016. I would also like to thank Professor Ahn Suk-kyun, Professor Choi Sungyoung for providing me opportunities to collaborate on interesting projects and continuously expand my horizon of knowledge. Thank you to Professor Park Tae Eun for not only being an instructor, a collaborator but also an inspiring example of a resilient and passionate female scientist.

While working on my research, I made many friends, whose supports were fuel to my growth in the past couple of years.

To Amanzhol, thank you for being my academic and life advisor, regardless of the topics, your insightful advice would always help me get back on my feet and push harder. You are my ride or die and I know for a fact that we would always have each other's backs no matter how far we are apart. Words cannot describe how much I am grateful for you, and for that, you deserve to be the Godfather of my future children.

To Suhyun, Minseok, Jungwon, and Brian, thank you for being my enthusiastic colleagues. I learned a great deal while working closely with you guys. Your feedback sharpened my thinking and brought my work to a higher level.

To Bonghwan, Sungjin, Ji-ung, Sim seonsengnim, and Professor Kwon, thank you for caring for me. You will always be a second family in my heart.

To my dear friends Sasha, Madina, I adore you girls so much and thank you for being by my side since undergraduate time. Together with Anchik, Almas, and Kat, we had two amazing (and safe) trips amid the crazy Corona pandemic and I would never forget these memories. I wish we could come together one day and have an adventurous trip again.

My special thanks go to my boyfriend, Valentyn Visyn. Your endless love, support, humor are treasures. Thank you for believing in me even when I doubt myself the most. Thank you for the stimulating discussions on anything and everything. I love our phenomenon food tour and consistent sessions of rowing, hiking, cycling, skateboarding, (attempted) pull-ups. They were indeed happy distractions to rest my mind outside of research. "Don't know where the path leads but happy to walk with you".

Quoting all of my other friends would be too long, but thank you and I love you all.

My biggest thank-you is for my family. Mom, dad, and Hieu, you are the reason I choose to keep my head up and move forward. Your relentless love is everything that made me who I am today. I know I can be quite a handful sometimes but deep down I am forever grateful and proud to call you guys my family. I promise I love you so much more than you will ever know.

Lastly, I would like to thank myself. Thank you for stop self - sabotaging and instead open up to the growth opportunities every day. With so much uncertainty to come in the future, I owe it up to my future self to work harder, dig deep, constantly edit self-identity, and make my past self proud of who we have become. For that, I say thank you.

